

## Chapter 13

# ADVANCES IN EXTERNAL BEAM RADIATION THERAPY

## *Towards Image-Guided and Adaptive Radiotherapy Using Multimodal Imaging*

Todd McNutt<sup>1</sup>, Michael R. Kaus<sup>2</sup>, Lothar Spies<sup>2</sup>

<sup>1</sup>Johns Hopkins University, Baltimore, MD, USA; <sup>2</sup>Philips Research, Hamburg, Germany

**Abstract:** Radiation therapy has advanced in the last decade fueled by the advancement of dose delivery (3D conformal, IMRT), computer processing, and medical imaging. Image processing techniques such as model-based image segmentation and deformable registration are becoming efficient enough for a clinical setting. Biological modeling based on nuclear medicine imaging is needed to provide a quantitative understanding of tumor biology and enable to identify regions of the tumor resistant to radiation, thereby, warranting a higher dose level. These imaging and processing techniques promise to advance radiotherapy with the ability to monitor the course of treatment by enabling image-guided radiotherapy and adaptive radiotherapy.

**Keywords:** Image guided radiotherapy, adaptive radiotherapy, ART, IMRT, molecular imaging, biological modeling, deformable image registration, image segmentation

## 1. INTRODUCTION

Cancer is the second leading cause of death in the industrialized countries and the only major disease for which death rates are increasing. The demand for cancer care will increase over the decade as the aging of the baby boomer population drives a dramatic increase in the incidence of many cancers.

Approximately 60% of cancer patients are treated with external beam Radiotherapy (RT) at some point during management of their disease. The main goal of RT is to maximize the dose to the target while limiting the dose

to nearby healthy organs ('risk organs'), in order to improve control of tumor growth and limit side effects.

Radiation therapy is primarily used to treat cancer by locally targeting radiation to the diseased tissue. Radiation beams are produced by medical linear accelerators. These devices are mounted on a gantry with a rotating couch to allow for many beam directions to be focused on the target volume. Sparing of normal tissues is accomplished in two fundamental ways: Geometric avoidance of normal tissues is accomplished by directing multiple beams at the target, thus delivering a high dose where the beams intersect at the target, and a relatively lower dose outside of the intersection. Biological sparing of normal tissue is accomplished by fractionating the therapy over several weeks, irradiating daily. The tumor tissue lacks repair mechanisms to repair DNA damage from the radiation, whereas normal tissues can repair minor DNA damage. Therefore, by fractionating the treatment, normal tissues are provided time to repair, thus biologically sparing the normal tissue.

In the late 1980s and 90s Computed Tomography (CT) based treatment planning became available due to the increased performance of computers. Both the imaging capabilities and the ability to compute radiation dose distributions on CT provided the framework for the modern 3D Radiotherapy Treatment Planning (RTP) system. These systems provide clinicians the ability to truly visualize and plan the treatments considering the true 3D nature of the problem.

Today, the current workflow for a patient begins with a CT simulation where the patient is immobilized with body molds and/or head masks. A CT scan is acquired and the patient is marked for repeated alignment with localization lasers in the treatment room. The treatment planning is then performed on the CT scan where beam geometries, energies, and collimation are determined, and the resultant dose distribution is computed. The treatments are then performed daily for several weeks. During the course of treatment, different imaging modalities are used to monitor the geometric setup of the patient to verify constancy in the patient position.

There have been many advances in the techniques used to deliver the treatment. Intensity Modulated Radiotherapy (IMRT) has allowed for each beam to be modulated, enabling dose distributions to carve out the target volume and spare normal tissues in the millimeter range. Several techniques and strategies have evolved and are in use today.

The research described in this chapter focus on the ability to accurately predict the dose and to precisely deliver the radiation to conform the dose to the target volume utilizing IMRT; the improvement in target and critical structure definitions through the use of multi-modality imaging; and the tools to enable the monitoring of the course of treatment to support image

guided radiotherapy (IGRT) which provides daily alignment of the patient with soft tissue target volumes, and adaptive radiotherapy (ART) which provides the monitoring the treatment through repeat imaging for decision support on modifying the treatment strategy.

## 2. INTENSITY MODULATED RADIOTHERAPY

IMRT is a method to determine the optimal beam intensity pattern for each beam to deliver the dose distribution specified by a set of treatment objectives and constraints. Under IMRT, the paradigm of RT changes from specifying beam directions and apertures, to one where one specifies dose or biology based treatment objectives and the computer will optimize the modulated beam intensities to best deliver the treatment<sup>1</sup>.

A typical target objective would be to deliver a uniform dose of 60 Gy in 30 fractions, and a typical critical structure objective would be to keep the dose below 25 Gy in more than 70% of the volume of the structure. Figure 13-1 shows a typical IMRT treatment.

The process of IMRT utilizes an inverse planning strategy that iteratively optimizes the intensity pattern of each beam to deliver the desired dose distribution defined by the objective functions. The intensity pattern of a beam is represented by a matrix of beamlets, each being a parameter of the treatment. The optimization process begins by initializing the intensity map (beamlets) of each beam to expose the target objective. Then the dose is computed for the set of beams. The treatment objective is evaluated, and the derivative of the objective with respect to each beamlet is determined. A new intensity map for each beam is determined by the optimization, and the dose is recomputed. This process is repeated until the improvement in the treatment objective between iterations is small indicating convergence to an ideal solution of intensity modulation.

Accurate dose calculation for RT is quite time consuming and is a difficult challenge for efficient IMRT planning. The convolution/superposition (C/S) dose engine in the Pinnacle<sup>3</sup> treatment planning system requires approximately 20 seconds per beam on a SunBlade 2000. This dose engine is quite accurate<sup>2-9</sup>, but lacks the speed required for during IMRT optimization. In order to maintain the accuracy of the C/S method, and gain the speed required for IMRT, the Delta Pixel Beam dose computation method was developed<sup>10</sup>. This method uses a high-speed pencil beam dose computation method to get close to the desired solution in early iterations of the IMRT optimization. Then the C/S method is used to compute the dose for the interim solution. Following the C/S computation, the pencil beam method is used to modify the dose based on the change in intensity of the

beam, leaving the majority of the dose computed by the more accurate C/S method.

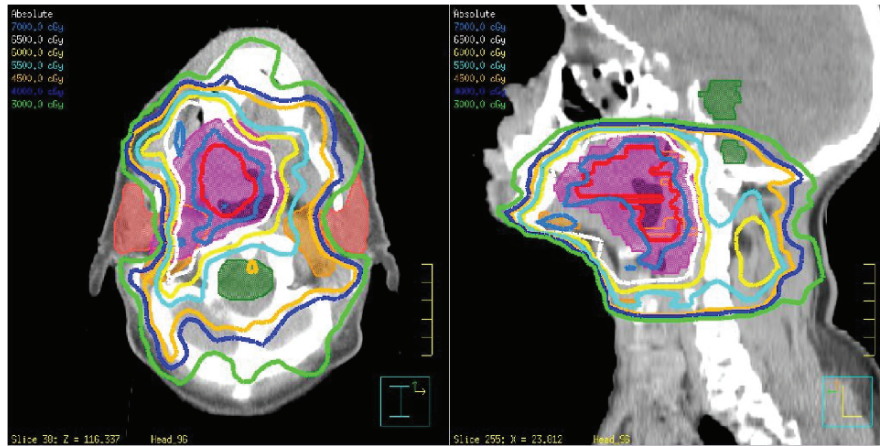


*Figure 13-1.* A 9-field IMRT treatment plan designed to deliver 60 Gy to the target volume (purple) and to spare the dose to the parotid glands (red) and the spinal cord and brainstem (green). The beams are equispaced in angle around the patient.

Once the intensity pattern of each beam is determined, it is converted into deliverable shapes by a multi-leaf collimator (MLC). Each beam will then be defined as a series of apertures defined by multiple MLC segments. Medical linear accelerators are equipped with MLC and deliver the set of MLC shapes automatically.

Newer methods in IMRT implemented in the Pinnacle<sup>3</sup> planning system include the ability to optimize the positions of each leaf of the MLC for each segment directly, rather than optimizing an intensity distribution for each beam, then later converting it to a set of MLC segments. By optimizing the leaf positions directly, the loss in desired treatment objective is reduced in the process.

IMRT provides a technique to conform the dose distribution tightly around a target volume while sparing the normal tissues. With this ability, the uncertainty in RT has been shifted to our ability to determine the desired target volumes, and the change in targets and critical structures over the course of RT.

### **3. MULTI-MODAL IMAGE PROCESSING TOOLS FOR TARGET AND STRUCTURE DEFINITION**

Understanding the use of multi-modal image-based information for treatment design is an area of intensive research around the world. The contouring of risk organs and the target area in medical images is a fundamental planning step to optimize treatment parameters. Today, contours are drawn manually (with a mouse) on every image slice, which is an extremely time- and labor-intensive task. Particularly in the head and neck the process may take several hours. The merits of IMRT can only be exploited if this type of segmentation is achieved. The integration of additional image-based information acquired weekly or even daily into the RTP process will lead to an additional substantial increase in data and workload by an order of magnitude or more. Automated image segmentation technology is necessary to automatically contour risk organs and the tumor in order to make the improved process clinically feasible.

Target definition based on the structural appearance of the tumor in CT has limited accuracy in determining the true extent of the disease, and does not allow assessment of morphology and biological changes in response to fractionated treatment. For example, PET/CT promises to improve throughput and accuracy for head and-neck RT planning by minimizing the uncertainty of contouring by the identification of metabolically active areas in PET, while CT provides high resolution and anatomical context to address non-tumor-specific uptake in PET. Recent studies have used CT against Magnetic Resonance Imaging (MRI) or PET alone rather than together with registered structured imaging, and the current clinical practice is to draw contours on one modality and transfer the contours manually to the planning CT. The optimal technique for fusing image data to compensate for inconsistencies between contours of different data sets remains controversially debated. Reproducible strategies for fusion of multi-modal contouring results and identification of conditions that exceed automated segmentation capacity are required.

Novel imaging agents such as fluoromisonidazole, [ $^{18}\text{F}$ ] FMISO and others are becoming more widely available and are gaining clinical importance for radiotherapy applications<sup>11</sup>. These novel tracers probe deeply into the biological and molecular characteristics of a cancer. The tracer FMISO, for example, is a PET tracer that selectively binds to cells, which suffer from an undersupply of oxygen. The importance with respect to radiotherapy planning stems from the fact that so-called hypoxic cells may survive a radiation dose, which is lethal to cells with normal oxygen supply. This has wide-reaching clinical consequences, which will prompt molecular imaging guided targeting of cancers on sub-tumor level.

In this section key technologies required to pursue this strategy comprising segmentation, deformable registration and biological modeling are addressed.

### 3.1 Segmentation and deformable registration approaches

**Image segmentation**, at any level of automation or trained operator interaction, is difficult due to insufficient tissue contrasts, imaging artifacts, and the high inter- and intra-individual variability in shape and appearance of structures in the human body. Research efforts in image analysis and processing resulted in a well-established statement that segmentation of difficult cases cannot be done using image content alone, and some additional information is required<sup>12,13</sup>.

A way to provide additional information to a segmentation algorithm is the use of prior knowledge about the shape of structures<sup>14</sup>. In medical image analysis, prior knowledge is represented, for example, in the form of an organ model, which includes information about both its shape as well as an organ-specific set of parameters specifying intensity range, gradient magnitude and direction, etc. When taking spatial relationships between different organs into account, this paradigm can be extended to organ constellations and even to whole regional anatomical atlases covering all structures of interest in particular body parts, which can automatically be adapted to the anatomy of individual patients.

Only few methods in the domain of automated organ segmentation for RTP that provide efficiency gain have been quantitatively proven to be accurate and robust so far. One can distinguish between three basic strategies in approaching this challenging problem: automation of 2D contouring aimed at robust detection of organ boundaries in 2D slices<sup>15</sup>, 3D approaches based on deformable organ model adaptation<sup>16,17</sup>, and methods based on adaptation of deformable atlases (images with labeled anatomy) to patient-specific image data<sup>18</sup>.

Automated 2D delineation does not require substantial changes in the workflow compared to manual contouring to which the physicians are used. On the other hand, 3D shape context is not used at all by these methods, and this may negatively influence their robustness. In contrast, 3D delineation tools are potentially much more productive, since they simultaneously operate in several slices. Methods based on volumetric deformable atlas adaptation may be very useful, e.g. for delineation of ‘invisible’ structures, e.g. in the head and neck area. However, the results of delineation are dependent on the robustness of the image modality at hand, the underlying image registration algorithm and the validity of the deformation model.

**Deformable image registration** has been studied since the early 80's<sup>19</sup> and for many years, brain surgery and neurosciences have been the driving applications for developing an abundant number of techniques<sup>20</sup>. Despite the significant progress that has been made, deformable registration is still not clinically accepted and remains a challenging problem.

Registration algorithms are categorized into non-parametric and parametric methods<sup>21</sup>. In the non-parametric case the displacement-vector is estimated for each voxel. The reduced complexity in parametric approaches leads to efficient computation times, at the cost of fidelity in describing deformations. A classical example is landmark registration<sup>22</sup>, where the new position for each voxel is interpolated or approximated from a given set of irregularly distributed points.

Another important choice is the deformation model, which can be purely geometric or physics-based. If the deformation process is due to physical processes, like in intra-patient registration, the use of physics-based deformation models aiming at describing real deformations may be advantageous over purely geometric transformations. Physics-based models are usually based on numerical<sup>23</sup> or analytical<sup>24,25</sup> solutions of the underlying equations of continuum mechanics.

A further classification of the registration techniques is the division into landmark-based, surface-based, and voxel-based methods. The first two groups provide the correspondences in the registered images between certain geometric entities, e.g. point landmarks or surfaces. The third group of methods maximizes voxel-based similarity between the images, i.e. information from the whole images contributes to the result.

In radiotherapy imaging, surface-based registration methods appear to be advantageous over voxel-based approaches. Surfaces of the relevant anatomical structures are available as output of the organ contouring. Based on this information, elastic tissue properties are assigned to the corresponding image regions<sup>26</sup>. Voxel-based image registration is difficult if the grey-value appearance of corresponding anatomical structures is not similar according to the definition of the similarity measure. This may not be the case in 4D CT of the thorax<sup>27</sup>, but is more severe in longitudinal imaging of e.g. the rectum, where the gray-value appearance constantly changes due to peristalsis.

### **3.2 Biological modeling**

As soon as functional or molecular images, such as PET or SPECT, and anatomical images are properly registered, the biological parameters relevant for defining a treatment, such as the radio-resistance across a tumor, have to be extracted. In the case of glucose metabolism as measured with FDG-PET

this is not problematic. FDG, an analogue of glucose, accumulates in most tumors in a greater amount than it does in normal tissue, because tumor tissue growing faster and sugar uptake is thus greater.

It is best clinical practice to quantify glucose metabolism by calculating a so-called standard uptake value (SUV). SUV is the FDG-PET signal in a specific pixel or region divided by the amount of administered tracer and the patient's weight. The normalization shall eliminate the effect of patient size and weight on the detected signal. It provides a semi-quantitative measure to enable a better differentiation of an individual disease. It further enables a comparison of disease grades between different patients.

However, for tracers, which feature more complex reaction patterns, such as hypoxia imaging with FMISO, and which probe deeper into the molecular pathways of the tissue, a simple normalization does not always provide enough specific information. In such cases a more sophisticated modeling is wanted. Then uptake rates, reaction rates, residence times and washout-rates, which are not directly accessible from the images, need to be considered.

A pharmacokinetic analysis applied to time series of functional images can help quantify these parameters<sup>28</sup>. This technique deploys mathematical models, which describe the interactions of the tracer molecule with the tissue in time. The tissue is subdivided into compartments, which have by definition a similar tracer concentration-time behavior. Transfer of tracer from one to the other compartment and reverse is modeled via exchange rates.

These exchange rates often represent important kinetic information, e.g. the trapping rate of metabolized FMISO correlates with oxygen content, which are estimated in a consecutive optimization process by fitting measured time-activity curves to the model. Performed on a per voxel basis, this results in so-called parametric maps. Figure 13-2 shows a parametric map quantifying hypoxia in a lung cancer superimposed to an FMISO-PET image of the whole thorax region sampled at 2 hours after tracer injection. The modeling engine has been integrated into a Pinnacle<sup>3</sup> (Philips Medical Systems, Milpitas, Ca) research prototype ('BioGuide').

Once parametric maps of the relevant parameter are available, the transition to a dose has to be made. Radiobiological models can guide dose prescription and provide a means to optimize dose with respect to tumor cell kill and reduction of collateral damage<sup>29</sup>. Very recently a theoretical framework has been presented to quantitatively incorporate the spatial biology data, such as parametric maps, into IMRT inverse planning<sup>30</sup>. This or a similar framework in combination with parametric maps can be used to guide dose escalation dose to sub-tumor volumes while keeping the dose to critical structures at minimum. This could be a step further towards a safer and more effective radiotherapy.



#### **4. IMAGE GUIDED AND ADAPTIVE RADIOTHERAPY**

In conventional RTP, risk organs and target areas are defined based on information that is currently limited to a single 3D anatomical CT image data set acquired at the onset of treatment design. This concept results in significant treatment uncertainties with irradiation of risk organs and reduced tumor coverage, see e.g. Mageras<sup>31</sup> and Chen<sup>32</sup> for review.

Natural processes in the body and response of normal and target tissue to the treatment result in significant inter- and intra-fractional geometrical changes. Intra-fractional geometric change occurs during radiation delivery due to breathing, cardiac motion, rectal peristalsis and bladder filling. Interfractional geometric change occurs in the extended time frame of fractionated radiotherapy (4-6 weeks), due to digestive processes, difference in patient setup, and treatment response like growth or shrinkage of the tumor or nearby risk organs (e.g. the parotids in head and neck treatment). These changes are only taken into account by population-based ‘uncertainty’ margins around the target area, which are often excessive and are applied to the structures identified before the therapy begins.

The concepts of adaptive radiotherapy (ART) and image-guided radiotherapy (IGRT) provide methods to monitor and adjust the treatments to accommodate the changing patient. ART is an off-line approach where the anatomical and biological changes are monitored over the course of treatment, and the treatment is modified when significant changes are identified. IGRT is typically an on-line concept where the patient or treatment plan is shifted or modified for each treatment. Both concepts require advanced image processing tools in order to be successful in clinical practice.

Additional imaging during the weeks of treatment is key to better understand and model these uncertainties. CT or kV cone-beam CT integrated into the treatment unit can provide patient-specific image-based quantitative surrogates of geometrical changes on the onset of a treatment fraction. Using the complementary strength of multi-modality imaging such as MRI providing superior soft-tissue contrast, and functional or molecular imaging such as PET, SPECT, MRI/MRS, can lead to improved target definition, and better understanding of the biological variations within the tumor that may affect response to the treatment. Finally, additional multi-modal imaging over the course of the treatment enables monitoring of target change over the course of therapy.

Integrating several image acquisitions over the course of treatment provides surrogates to compensate the change of risk organs and target areas. Besides the efficiency issue related to contouring, multi-modal image

analysis requires estimating the correspondence between each voxel element of the multiple planning images. Estimating correspondences requires dedicated deformable image registration algorithms.

#### **4.1 Concept for automated segmentation and deformable registration for adaptive IGRT**

In order to manage a series of images from the same patient, an integrated concept of automated image segmentation and deformable image registration, in which an operator is provided with efficient algorithms that compute in the order of seconds, and a set of interactive tools to quickly access segmentation and registration results, and correct problematic areas if required.

The concept of automated organ segmentation proposed is a particular form of adapting deformable surface models<sup>33</sup>. Flexible surfaces are adapted to object boundaries by optimization of a measure expressing the goodness of the fit to image data in combination with certain constraints controlling the geometric properties of the surface.

To reduce the need for accurate initialization and reduce the problem of attraction to false boundaries, a framework of shape-constrained deformable model adaptation was developed<sup>34</sup>, where prior knowledge obtained by a learning process<sup>35</sup> is embedded into an elastically deformable triangular mesh to compensate for the lack of reliable image content.

In the context of shape-constrained deformable models, a generic shape model is provided for each anatomical structure, i.e. a bladder model, a liver model, a lung model, etc. Since different structures consist of different tissue types (bone, soft tissue) with different imaging characteristics (grey value, contrast), organ-specific image features are used to diminish the risk for the model to be attracted by false image structures<sup>16</sup>.

In an experimental validation study with 40 patient datasets, Pekar et al.<sup>16</sup> demonstrate that the method is suitable for clinical use for risk organs in the prostate area, i.e. bladder, rectum, and femoral heads, and significantly reduces the time for organ delineation compared to manual segmentation, with comparable segmentation accuracy in the order of 1-1.7 mm mean error. An example of the study is shown in Figure 13-3.

The ability to use deformable models efficiently for the segmentation of CT time series for prostate treatment planning was evaluated in Kaus et al.<sup>36</sup>. In order to increase the degree of automation and reduce the amount of interaction with each 3D volume in the image time series, an automated initial positioning strategy was developed based on the propagation of adapted surface meshes from one 3D image dataset to the next. The feasibility of this 4D approach was tested on a CT image time series taken

from a single subject containing 16 3D CT datasets obtained at different days before and during treatment. Quantitative analysis demonstrated comparable results to the 3D interactive method for the femur and the bladder.

In another study, the tools were applied to the problem of risk organ segmentation in 4D CT imaging for lung tumor treatment planning<sup>37</sup>. The assessment was based on the 8 breathing phases of a patient's 4D CT dataset. Patient-specific models for the lungs, the heart, the spinal cord and the esophagus were generated by a clinical user on a Pinnacle<sup>3</sup> research prototype installed in the hospital, by manual contouring and triangulation of the first phase. The mesh adaptation algorithm was then carried out on the remaining 7 phases without further interaction. Accurate results were reported for all structures except for the esophagus, which is surrounded by soft tissue of similar grey value appearance.

When applying surface-based segmentation in a primary and a secondary dataset, a boundary mapping between the organ surfaces is automatically established through the correspondences between the mesh vertices. This information can be used for deformable image registration<sup>38</sup>. Essentially, a point-based deformable registration scheme is used, where the vertices of the triangular meshes act as corresponding control points. A spline function maps each control point in one image to the corresponding control point in the other image, while interpolating the mapping at all intermediate locations in the image.

Since the computation time increases linearly with the number of control points, only a subset of mesh vertices that is evenly distributed over the entire surface is used for the deformation. A reduction in the number of vertices (e.g. from 4000 to 80) reduces the computation time from hours to seconds on standard PC hardware with comparable surface registration accuracy.

In order to be clinically acceptable, the automated tools compute results in the order of seconds. Secondly, they support efficient editing, allowing the operator to quickly access and correct problematic areas if required. The user is provided with the ability to manipulate the model, thus interacting with both the segmentation of a structure and the deformable registration of a secondary image. For example, automated mesh adaptation, manual deformation of the mesh proportional to the translation of the mouse pointer, and re-sampling of a secondary image according to an updated deformable transform.

In contrast to manual slice-wise delineation, complete organ segmentation is possible within a few minutes. In addition, delineated structures are represented by smooth 3D shapes and not by stacked 2D

slices, which avoids the common ‘Christmas tree’ effect by providing smooth surfaces.

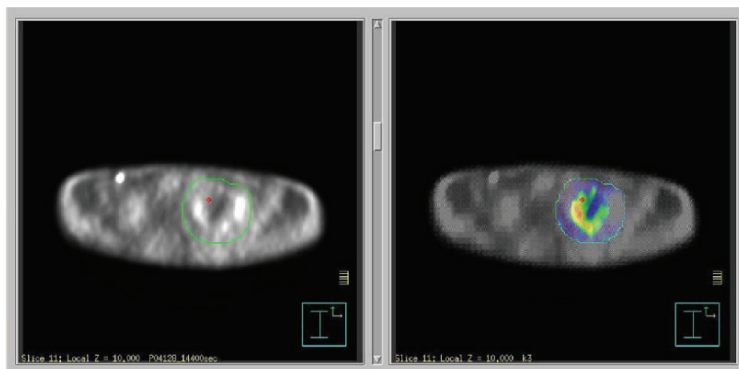


Figure 13-2. BioGuide plug-in is a research application running under Pinnacle3. The plug-in features a pharmacokinetic modeling engine and radiobiological modeling to improve target definition of an individual disease. Left window: FMISO-PET late time image with target contour in green. Right window: Same FMISO-PET image but with the corresponding parametric map (color coded) representing hypoxia for the tumor region superimposed.

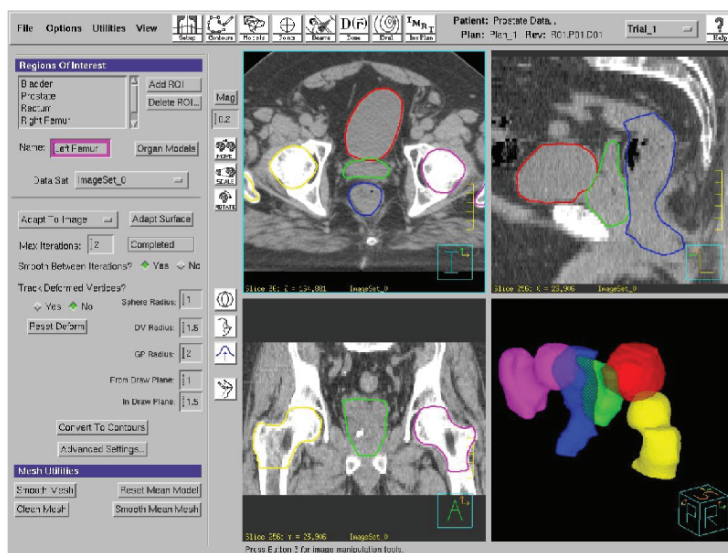


Figure 13-3. 3D model-based segmentation in CT of the target and the organs of risk. The image shows three orthogonal cross-sections, the contours where the surface meshes intersect the cross-sections (femur heads, bladder, rectum, prostate), and a rendering of the 3D surface models.

Unlike most voxel-based deformable registration schemes, surface-based registration is computationally efficient. In addition, because the deformation is controlled by surfaces that can be edited by an operator, it is possible to interact with the deformation algorithm, which is important in the context of clinical acceptance of a deformable registration algorithm.

Another important advantage of the presented approach is its generality. The organ database is currently being extended to other treatment areas such as breast, liver, lung, head and neck. Potentially, the method can be applied to other imaging modalities by using the principle of organ-specific image features<sup>39</sup>.

## **4.2 Validation concepts for adaptive radiotherapy**

In-treatment room kV cone-beam CT (CBCT) imaging is an emerging technology, which has still not reached the image quality of a conventional CT imaging regarding spatial resolution and soft tissue detectability.<sup>40</sup> Hence image processing techniques, which provide good registration and segmentation for conventional CT time series, may not be directly applicable to IGRT based on cone-beam volumetric imaging.

A test suite was designed to simulate the quantitative impact of CBCT imaging quality on the performance of image registration and segmentation techniques used to correlate treatment time images with planning images.<sup>41</sup> The result is measured with respect to improvements of the dose volume histograms. The main components of the test suite are:

- A simulation engine to transform the grey-values of conventional CT images to better match the imaging characteristics of CBCT, including effects such as beam quality, residual scatter, residual beam hardening, simulation of defect pixels, truncation, flat panel detector noise.
- The segmentation and registration algorithms such as described above.
- An inverse planning dose engine to create treatment plans and associated dose distributions based on the delineated target and organ at risks.
- A plan evaluation tool to create dose-volume histograms.

A first result suggested that rigid registration works robustly on CBCT even under low dose conditions. Moreover, an adaptation of the plan using a rigid correlation already improves the dose volume histogram.

## 5. SUMMARY

Radiation therapy (RT) has seen several advances in the past decade. Many improvements in computers, imaging and image post-processing technology have fueled much of these advancements. Sophisticated dose computation, 3D visualization and planning tools were enabled in software systems such as Pinnacle<sup>3</sup>. Intensity modulated radiotherapy was the next logical step and has provided the clinicians the ability to carve out dose distributions to treat desired targets while sparing normal structures.

The next round of advancements in RT include adaptive radiotherapy and image guided radiotherapy where the image based monitoring of the patient and treatment will enable correction of the treatment while the patient is on the table, or monitoring of the anatomical or biological changes in the patient prompting re-planning of the treatment if necessary.

These new techniques require substantial advances in image processing in the areas of model based image segmentation, deformable image registration and biological modeling. These tools will enable the evaluation of anatomical and biological changes in the patient and the accumulation of the true delivered doses to the tissues undergoing deformations during the course of RT.

Further evaluation of the biological and functional properties of the tissues in RT is enabling better definition of target volumes and improved knowledge of the effects of RT on biological function. Molecular imaging techniques have the potential to identify hypoxic regions of tissues, which are known to be resistant to RT, enabling the clinician to consider this in the prescription of doses. The knowledge of molecular imaging combined with intensity-modulated radiotherapy (IMRT) will give the clinician the ability to tailor the dose distribution to the anatomical target volumes as well as boost the dose to regions that are identified as either resistant to radiation, or regions known to contain high densities of tumor tissue.

As these techniques advance, radiotherapy departments will need to manage image-based data at an ever-increasing rate. Computers will continue to play a large role in advancing the practice of RT as well as other areas of medicine.

## REFERENCES

1. J. Löf, H. Rehbinder, T. McNutt, and S. Johnson, P3IMRT Inverse planning optimization, *White Paper Publication, ADAC Laboratories (Philips)*, (Milpitas, CA 2002).
2. R. Mohan, C. Chui, and L. Lidofsky, Energy and angular distributions of photons from medical linear accelerators, *Med Phys* **12**, 592-597 (1985).

3. T.R. Mackie, J.W. Scrimger, and J.J. Battista, A convolution method of calculating dose for 15-MV Xrays, *Med Phys* **12**, 188-196 (1985).
4. T.R. Mackie, A.F. Bielajew, D.W.O. Rogers, et al., Generation of photon energy deposition kernels using the EGS Monte Carlo code, *Phys Med Biol* **33**, 1-20 (1988).
5. T.R. Mackie, P.J. Reckwerdt, T.R. McNutt, et al., Photon dose computations, *Proc AAPM Summer School, AAPM-College Park, MD* (1996).
6. A. Ahnesjo, P. Andreo, and A. Brahme, Calculation and application of point spread functions for treatment planning with high energy photon beams, *Acta Oncol* **26**, 49-56 (1987).
7. N. Papanikolaou, T.R. Mackie, C. Meger-Wells, et al., Investigation of the convolution method for polyenergetic spectra, *Med Phys* **20**, 1327-1336 (1993).
8. M.B. Sharpe and J.J. Battista, Dose calculations using convolution and superposition principles. The orientation of the dose spread kernels in divergent Xray beams, *Med Phys* **20**, 1685-1694 (1993).
9. T.R. McNutt, T.R. Mackie, P. Reckwerdt, et al., Calculation of portal dose images using the convolution/superposition method, *Med Phys* **23**(4), 527-535 (1996).
10. T.R. McNutt, Dose calculations Collapsed cone convolution and delta pixel beam, *White Paper Publication, ADAC Laboratories (Philips), Milpitas, CA* (1999).
11. J.D. Chapman, J.D. Bradley, J.F. Eary, et al., Molecular (functional) imaging for radiotherapy applications an RTOG symposium, *Int J Rad Onc Biol Phys* **55**(2), 291-301 (2003).
12. M. Kass, A and Witkin, D. Terzopoulos, Snakes active contour models, *Int J of Computer Vision* **1**(4), 321-331 (1988).
13. D.L. Collins, T.M. Peters, W. Dai, et al., Model-based segmentation of individual brain structures from MRI data, *Proc Vis Biomed Comp*, 10-23 (1992).
14. T.F. Cootes, A. Hill, C.J. Taylor, et al., The use of active shape models for locating structures in medical images, *Imag Vis Comp* **12**(6), 355-366 (1994).
15. L.S. Hibbard, Region segmentation using information divergence measures, *Proc MICCAI*, 554-561 (2003).
16. V. Pekar, T.R. McNutt, and M.R. Kaus, Automated model-based organ delineation for radiation therapy planning in the prostate region, *Int J Rad Onc Biol Phys* **60**(3), 973-980 (2004).
17. S. Pizer, P. Fletcher, S. Joshi, et al., Deformable M-reps for medical image registration, *Int J Comp Vis* **55**(2), 85-106 (2003).
18. P.F. D'Haese, V. Duay, R. Li, et al., Automatic segmentation of brain structures for radiation therapy planning, *Proc SPIE Medical Imaging*, 517-526 (2003).
19. R. Bajcsy and S. Kovacic, Multiresolution elastic matching, *Comp Vis Graph Imag Process* **46**, 1-12 (1982).
20. A. Toga (ed.), *Brain Warping*, (Academic Press, 1999).
21. J. Modersitzki, *Numerical methods for image registration*, (Oxford University Press, 2004).
22. F. Bookstein, Principal warps thin-plate splines and the decomposition of deformations, *IEEE PAMI* **11**, 567-585 (1989).
23. G. Christensen, R. Rabbitt, and M. Miller, Deformable templates using large deformation kinematics, *IEEE Trans Imag Process* **5**, 1435-1447 (1997).
24. M. Davis, A. Khotanzad, D. Flaming, et al., A physics-based coordinate transformation for 3D image matching, *IEEE Trans Med Imag* **16**(3), 317-328 (1997).
25. J. Kohlrausch, K. Rohr, and S. Stiehl, A new class of elastic body splines for nonrigid registration of medical images, *Proc BVM*, 164-168 (2001).
26. K. Brock, M. Sharpe, L. Dawson, et al., Accuracy of finite element model-based multi-organ deformable image registration, *Med Phys* **32**(6), 1647-1659 (2005).

27. T. Guerrero, G. Zhang, T. Huang, et al., Intrathoracic tumour motion estimation from CT imaging using the 3D optical flow method, *Phys Med Biol* **49**(2204), 4147-4161 (2004).
28. S. Huang, and M.E. Phelps, Principles of tracer kinetic modeling in positron emission tomography and audiography – principles and applications for the brain and heart, Raven Press, New York, 287-346 (1986).
29. G.G. Steel (ed), *Basic clinical radiobiology* (Oxford University Press, 2002).
30. Y. Yang, and L. Xing, Towards biologically conformal radiation therapy (BCRT) Selective IMRT dose escalation under guidance of spatial biology distribution, *Med Phys* **32**(6), 1473-1483 (2005).
31. G. Mageras (ed.), Management of target localization uncertainties in external beam therapy, *Seminars in Radiation Oncology* **15**(3) (2005).
32. G. Chen, T. Bortfeld (eds.), High-Precision therapy of moving targets, *Seminars in Radiation Oncology* **14**(1) (2004).
33. T. McInerney and D. Terzopoulos, Deformable models in medical image segmentation, *Med Imag Anal* **1**(2), 91-108 (1996).
34. J. Weese, M. Kaus, C. Lorenz, et al., Shape constrained deformable models for 3D medical image segmentation, *Proc IPMI*, 380-387 (2001).
35. M. Kaus, V. Pekar, C. Lorenz, et al., Automated 3D PDM construction from segmented images using deformable models, *IEEE Trans Med Imag* **22**(8), 1005-1013 (2003).
36. M.R. Kaus, T.R. McNutt, and V. Pekar, Automated 3D and 4D organ delineation for radiation therapy planning in the pelvic area, *Proc SPIE Medical Imaging*, 346-356 (2004).
37. D. Ragan, G. Starkschall, T. McNutt, et al., Semiautomated four-dimensional computed tomography segmentation using deformable models, *Med Phys* **32**(7), 2254-2261 (2005).
38. M.R. Kaus, V. Pekar, T.R. McNutt, et al., An efficient algorithm for image-based dose deformation and accumulation, *Med Phys* **32**(6), 1900 (2005).
39. M.R. Kaus, J. von Berg, J. Weese, et al., Automated segmentation of the left ventricle in cardiac MRI, *Med Imag Anal* **8**, 245-254 (2004).
40. D. Jaffray, Emergent technologies for 3-dimensional image-guided radiation delivery, *Seminars in Radiation Oncology* **15**, 15208-216 (2005).
41. M. Bal, L. Spies, and T. McNutt, Adapting treatment plan to organ motions and deformations using x-ray volumetric imaging, *Proc ESTRO*, abstract (2003).